Vibrational Spectroscopy at High Pressure of the Permanganate Anion Trapped in Potassium Bromide and Potassium Perchlorate Matrices

Mirela M. Barsan, Ian S. Butler,* and Denis F. R. Gilson*

Department of Chemistry, McGill University, 801 Sherbrooke Street West, Montréal, Québec H3A2K6, Canada

Received: January 16, 2006; In Final Form: March 11, 2006

The effect of high pressure on the resonance Raman spectra of the permanganate ion isolated in potassium bromide and potassium perchlorate matrices has been investigated at room temperature for pressures up to 50 kbar. The pressure dependences of the anharmonicity constants and harmonic frequencies have been determined from the overtones of the totally symmetric $\nu_1(A_1)$ mode of the permanganate ion. For both matrices, as the pressure increases, the anharmonicity constants decrease slightly, while the harmonic frequencies increase steadily. The effect of the potassium bromide phase transition from a face-centered to a body-centered structure was observed on the permanganate ion Raman spectrum at ∼24 kbar. The perchlorate matrix does not exhibit any phase transition under the experimental conditions used in this study.

Introduction

The nonresonance Raman spectrum of dark purple $KMnO_4$ in the solid phase and in aqueous solution has been the subject of several studies.[1,2] Kiefer et al.[3,4] developed a special rotating Raman sample device to overcome the well-known difficulty of measuring the spectra of colored compounds using visible lasers and observed the resonance Raman effect in both aqueous solution and solid $KMnO_4$.[5,6] The anharmonicity constant and harmonic frequency at ambient pressure for the symmetric stretching vibration, $\nu_1(A_1)$ of the T_d-symmetry MnO_4^- ion were obtained from its overtones. An alternative method of avoiding the heating of the $KMnO_4$ powder and its decomposition to manganese dioxide during the Raman measurements is the inclusion of the MnO_4^- ion in different crystalline environments, i.e., by matrix isolation,[7] and the MnO_4^- ion has been studied in a variety of host lattices such as KBr,[8−11] $KClO_4$,[12−15] RbBr,[16] CsI,[17] sodalite cages,[18] $[Ph_4P]^+$ salt,[19] and 18-crown-6 ether complex.[20] The resonance Raman excitation profiles of the totally symmetric $\nu_1(A_1)$ mode and its overtones for the MnO_4^- ion substituted in KBr,[10,11] or $KClO_4$,[12,13] have been extensively studied. The shift of the equilibrium Mn−O bond length for the permanganate ion was found to be 9.2 pm for the MnO_4^- anion embedded in a potassium perchlorate matrix. Moreover, Taiti et al.[14,15] have obtained the room temperature resonance coherent anti-Stokes Raman spectra of the ground and excited state of the $\nu_1(A_1)$ vibration for the MnO_4^- ion isolated in $KClO_4$. The values for the electronic ground- and excited-state wavenumbers of the $\nu_1(A_1)$ vibration of the MnO_4^- ion in a $KClO_4$ matrix,[13,14] which lead to the best fit between the excitation profiles, calculated using the Franck−Condon mechanism and the experimental data, are 846 and 740 cm^{-1}, respectively. Finally, Khodadoost et al.[21] have examined the effect of external pressure, up to 150 kbar, on the optical absorption and resonance Raman excitation profiles of the $\nu_1(A_1)$ mode and its first two overtones for the MnO_4^- dispersed in a matrix of $KClO_4$.

The goal of the present study was to use the resonance Raman effect to determine the pressure dependences of the anharmonicity constants and harmonic frequencies of $KMnO_4$ isolated in KBr and $KClO_4$ matrices. At ambient pressure and temperature, the KBr host matrix crystallizes in a face-centered cubic structure and presents the advantage of being inactive in Raman spectroscopy. In addition, the effect of a pressure-induced phase transition of the KBr matrix on the spectrum of the permanganate anion was observed. In the case of potassium perchlorate, the spectral analysis is more complicated because the perchlorate ion itself exhibits four characteristic Raman-active modes.

Experimental Section

Crystals of the permanganate ion trapped in KBr were prepared by adding $KMnO_4$ to an aqueous solution of KBr at room temperature. The solution was filtered and kept in a dark environment to avoid the formation of manganese dioxide. After slow evaporation of the water at room temperature, pink crystals of KBr doped with MnO_4^- were obtained. Crystals of the MnO_4^- anion isolated in a $KClO_4$ matrix were prepared following a method described in the literature.[14] This preparation was completed in a dark environment. The concentrations of the MnO_4^-, determined by UV−vis spectroscopy, were 2.5×10^{-5} and 1.08×10^{-5} M, respectively.

Raman spectra were recorded on a Renishaw 3000 monochromator system equipped with a Leica microscope, a charged-coupled detector, and 1800 lines/mm holographic grating. The excitation sources were Ar^+ (488, 514 nm) and He−Ne (633 nm) ion lasers. Prior to the measurements, a silicon wafer was used for the calibration of Raman spectrometer. The spectra were recorded using a long-working-distance 20× objective, a slit of 50 μm, and a laser power of 25 mW. The fitting of the Raman peaks was performed using GRAMS/32 software.[22] Wavenumbers are estimated to be accurate to at least ± 1 cm^{-1}.

Pressure was applied using a diamond anvil cell (High-Pressure Diamond Optics, Inc., Tucson, AZ) fitted with a pair of type IIA diamonds. The sample was placed, using an optical microscope, into the 300 μm hole drilled in the middle of a

* Authors to whom correspondence should be addressed. Phone: +1-514-398-6910 (I.S.B.); +1-514-398-6908 (D.F.R.G.). Fax: +1-514-398-3797. E-mail: ian.butler@mcgill.ca; denis.gilson@mcgill.ca

10.1021/jp060308y CCC: $33.50
Published on Web 04/15/2006

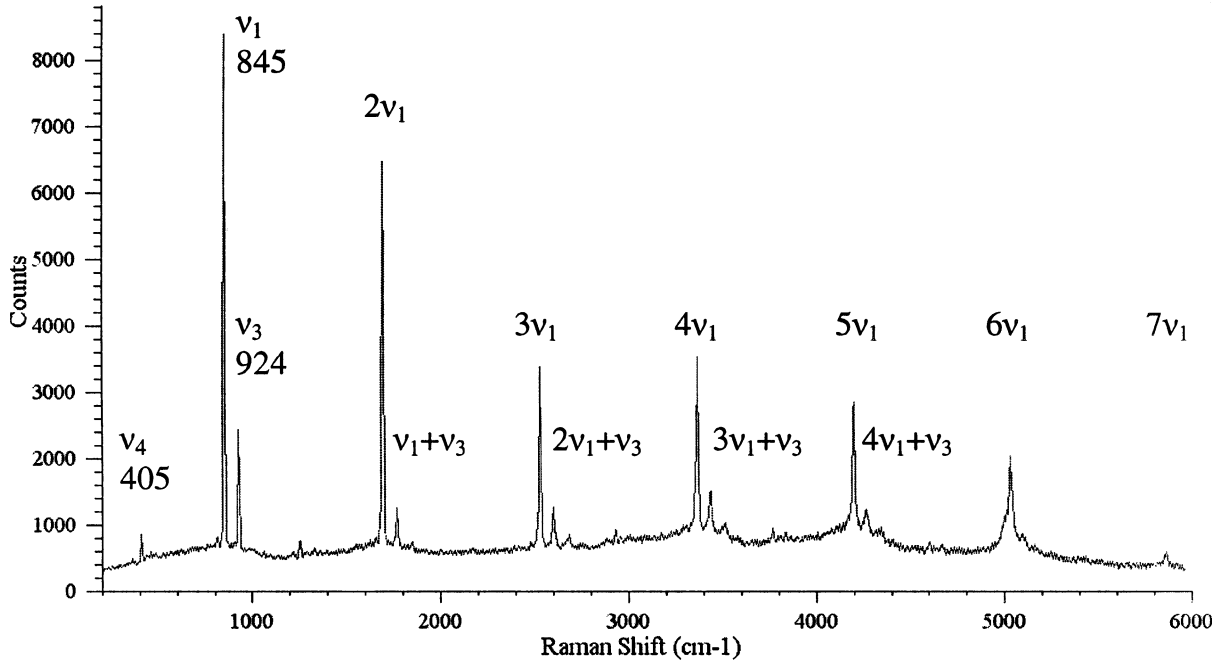

Figure 1. Resonance Raman spectrum of the MnO_4^- anion isolated in a KBr host lattice at ambient pressure (recorded on a microscope slide).

stainless steel gasket (7 mm × 7 mm × 270 μm) mounted between the parallel faces of the two diamonds. A microcrystal of ruby was added into the gasket. To ensure hydrostatic conditions a methanol/ethanol mixture (4:1) was incorporated into the gasket hole as well. The pressure measurements were performed using the R_1 line of ruby and a well-known calibration.[23]

UV−vis spectra were obtained using a Hewlett-Packard 8453 spectrophotometer furnished with cells with 1.0 cm path lengths. Spectral data of the aqueous solutions of the prepared crystals were collected from 200 to 1000 nm.

Infrared spectra, in the form of KBr pellets, were recorded at ambient pressure and temperature, using an ABB Bomem Fourier transform infrared spectrometer, at 1 cm^{-1} resolution. The spectral manipulations were made using the Win-Bomem Easy software.

All of the spectroscopic measurements reported in this paper were performed at room temperature.

Results and Discussion

Resonance Raman Spectra of the MnO_4^- Anion Embedded in a KBr Matrix. As a typical tetrahedral T_d-symmetry MX_4 species, the MnO_4^- ion displays four fundamental vibrational modes, all ($A_1 + E + 2T_2$) are Raman-active, and two of them ($2T_2$) are infrared-active. In crystalline $KMnO_4$, the very strong Raman band at 842 cm^{-1} is assigned to the totally symmetric stretching mode $\nu_1(A_1)$, the very weak peak at 349 cm^{-1} is attributed to $\nu_2(E)$, and the band located at 396 cm^{-1} is assigned to $\nu_4(T_2)$. The bands at 904 and 914 cm^{-1} are due to the triply degenerate mode $\nu_3(T_2)$,[3] which splits into two components by site symmetry. The infrared spectrum of the MnO_4^- ion shows only two absorption bands, located at 925 and 398 cm^{-1}, corresponding to the ν_3 and ν_4 modes.

The crystal structure of the $KMnO_4$ is orthorhombic with four molecules per primitive cell ($Z = 4$) and a space group *Pnma* with the following unit cell parameters: $a = 9.105(5)$, $b = 5.720(3)$, and $c = 7.425(4)$ Å.

To calculate the anharmonicity constant and harmonic frequency for a particular fundamental vibration of a compound, the experimental observation of a number of overtones is required. It is well established that the resonance Raman phenomenon will enhance the intensities of a particular fundamental mode and the progression of its associated overtones by several orders of magnitude. Because of the low concentration of the MnO_4^- ion in the host matrix, it is crucial to acquire resonance Raman spectra. The 514 and 488 nm argon laser lines fit an extremum of the fine structure of the electronic absorption spectrum, and the resonance Raman spectra of the MnO_4^- anion, isolated in the KBr host lattice, showed a progression of six overtones of the totally symmetric stretching mode, $\nu_1(A_1)$, with decreasing intensity but increasing half-bandwidth. With the He−Ne laser, operating at 633 nm, only one overtone of the $\nu_1(A_1)$ vibration could be detected. Figure 1 shows the resonance Raman spectrum of the MnO_4^- anion in a KBr environment obtained at ambient pressure using the 514 nm excitation line. In the low-frequency region of the spectrum, two narrow strong bands at 845 and 924 cm^{-1} as well as two much weaker bands at 405 and 361 cm^{-1} were observed and were assigned as $\nu_1(A_1)$, $\nu_3(T_2)$, $\nu_4(T_2)$, and $\nu_2(E)$, respectively. Furthermore, a progression of the six overtones of the totally symmetric mode $\nu_1(A_1)$ of the MnO_4^- anion in KBr environment was evident. In addition to these harmonics, a progression of combination bands ($n\nu_1 + \nu_3$) of the totally symmetric mode $\nu_1(A_1)$ and the antisymmetric vibration $\nu_3(T_2)$ was observed together with weaker progressions assigned to $n\nu_4$, $n\nu_3$ ($n = 1-4$), and combination bands $n\nu_1 + \nu_4$ and $\nu_1 + \nu_2$.

The infrared spectrum of the MnO_4^- anion in the KBr matrix shows two absorption bands, one strong at 925 cm^{-1} and the other one very weak at 397 cm^{-1} corresponding to the $\nu_3(T_2)$ and $\nu_4(T_2)$ modes, respectively.

The effect of high pressure on the Raman-active $\nu_1(A_1)$ and $\nu_3(T_2)$ modes of the MnO_4^- anion in the KBr environment is shown in Figure 2. Both vibrations shift to higher wavenumbers for pressures up to ~24 kbar, when the $\nu_1(A_1)$ mode decreases significantly in intensity and becomes very broad. At the same pressure, a new peak appears at 877 cm^{-1}. This is clear evidence of the occurrence of the pressure-induced phase transition in the KBr matrix. When the pressure is released, the initial Raman

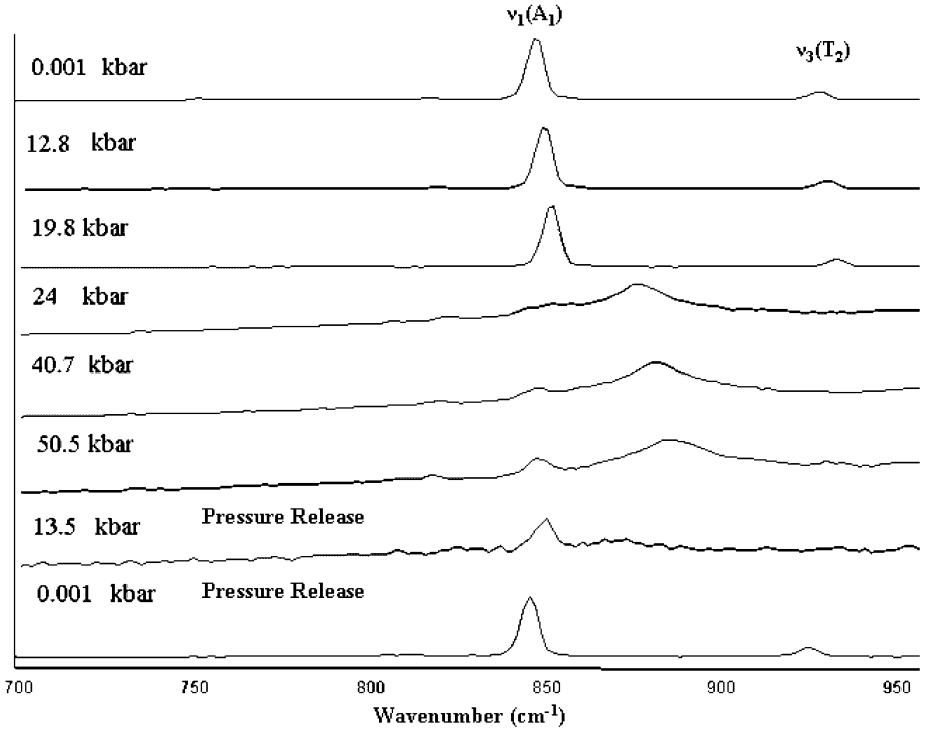

Figure 2. Selected Raman spectra as a function of pressure for the MnO_4^- anion in a KBr host matrix.

spectrum was obtained, indicating that the phase transition is reversible. Potassium bromide is known to undergo a first-order structural phase transition from a face-centered cubic NaCl-like (B1) structure to a body-centered CsCl-like (B2) one at about 17−19 kbar.[24,25] The investigation of the B1 ⇄ B2 transition was carried out by Slater[26] as early as 1924 and by Jacobs[27] in 1938 and is one of the simplest reconstructive first-order transitions known.

Applying an external pressure to a crystal leads to a compression of the unit cell resulting in an increase of the energies of the vibrational modes. This is an explanation for the observed shifts of the several modes toward higher wavenumbers, since the interatomic and intermolecular interactions increase as the separations become smaller. The wavenumber versus pressure plots for the $\nu_1(A_1)$, $\nu_3(T_2)$, and $\nu_4(T_2)$ fundamental vibrations are shown in Figure 3. Increasing the pressure up to ∼24 kbar had the following consequences: (i) the dν/dP value of the $\nu_1(A_1)$ mode (Table 1) changed from being positive (0.32 cm^{-1} kbar^{-1}) to negative (−0.16 cm^{-1} kbar^{-1}), (ii) a peak appeared at 877 cm^{-1}, and (iii) after 24 kbar, the $\nu_3(T_2)$ and $\nu_4(T_2)$ peaks disappeared. Owing to the very weak intensity of the $\nu_2(E)$ mode, even at ambient pressure, it was not possible to obtain the pressure dependence for this vibration.

The values calculated for the pressure sensitivities, dν/dP, indicate that the $\nu_1(A_1)$ and $\nu_4(T_2)$ modes showed the same pressure dependence (0.32 cm^{-1} kbar^{-1}), while that of $\nu_3(T_2)$ is much higher (0.51 cm^{-1} kbar^{-1}). This latter mode differs from the other normal modes by being the only one involving motion of the central atom Mn[28] and involves a greater displacement of the whole molecule.

Figure 4 illustrates the effect of the increasing external pressure on the bandwidth at the half-height of the totally symmetric mode $\nu_1(A_1)$. The bandwidth was constant, about 5.4 cm^{-1} up to 24 kbar, followed by a sharp increase to 22 cm^{-1} at 27 kbar. After this pressure, the $\nu_1(A_1)$ bandwidth decreased sharply. The increasing of the broadness of the $\nu_1(A_1)$ Raman band is a further indication that the crystal undergoes a phase transition as the peak is inhomogeneously broadened over the transition region.

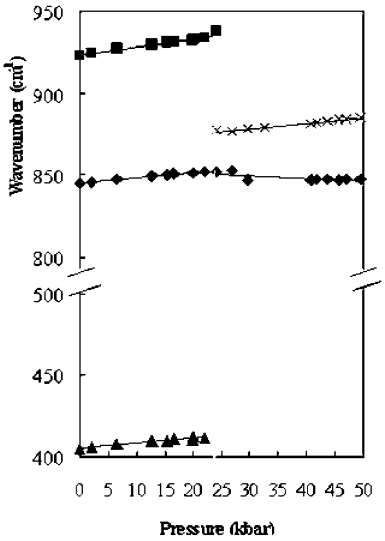

Figure 3. Pressure dependence of observed Raman modes for the MnO_4^- anion trapped in a KBr matrix: (◆) $\nu_1(A_1)$, (■) $\nu_3(T_2)$, (▲) $\nu_4(T_2)$, (×) new peak.

TABLE 1: Raman Fundamental Bands and Their Pressure Sensitivities for the MnO_4^- Anion Trapped in a KBr Matrix

ν (cm^{-1})	dν/dP (cm^{-1} kbar^{-1})	assignment
924	0.51[a]	$\nu_3(T_2)$
877	0.34[b]	new peak
845	0.32[a]	$\nu_1(A_1)$
	−0.16[b]	
405	0.32	$\nu_4(T_2)$

[a] Before phase transition. [b] After phase transition.

It should be emphasized that measuring the Raman spectrum through the diamond windows of the anvil cell reduces the intensity of the Raman bands, and consequently, some very weak

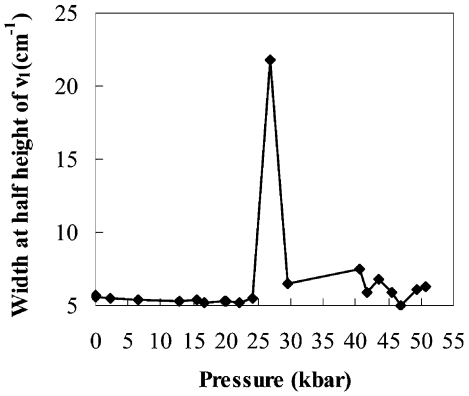

Figure 4. Bandwidth at half-height of the $\nu_1(A_1)$ mode as a function of pressure for the MnO_4^- anion insolated in a KBr host matrix.

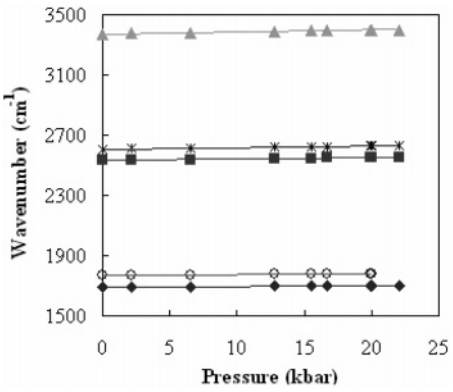

Figure 5. Pressure-induced shifts of the $\nu_1(A_1)$ overtones and $n\nu_1 + \nu_3$ combination bands of the MnO_4^- anion isolated in a KBr matrix: (◆) $2\nu_1(A_1)$, (■) $3\nu_1(A_1)$, (▲) $4\nu_1(A_1)$, (○) $\nu_1 + \nu_3$, (∗) $2\nu_1 + \nu_3$.

bands disappear. As a result, only the first three overtones of the $\nu_1(A_1)$ mode could be measured. These overtones and the combination bands shift linearly to higher wavenumbers up to ~24 kbar (Figure 5). At pressures above 24 kbar, these bands were not observable.

The Raman wavenumbers and the pressure dependences for the $\nu_1(A_1)$ overtones and the $n\nu_1 + \nu_3$ combination bands of the MnO_4^- ion in the KBr host lattice are listed in Table 2. The slopes of these higher-order Raman bands are very close to those obtained by adding the slopes of the corresponding fundamentals, shown in Table 1, i.e., the addition of linear functions, indicating small values for the cross terms in the anharmonicity expansion, eq 1.

The harmonic progression of a particular fundamental mode permits determination of the anharmonicity constant x_{11} and harmonic frequency ω_1. For an anharmonic oscillator the observed wavenumber, $\nu(n)$, is given by[28]

$$\nu(n) = G(n) - G(0) = n\omega_1 + x_{11}(n^2 + n) + n(x_{12} + {}^3/_2 x_{13} + {}^3/_2 x_{14}) \quad (1)$$

where $G(n)$ is the term value, n is the vibrational quantum number, and x_{1n} ($n = 2-4$) are cross terms. Neglecting the cross terms leads to the following expression

$$\nu(n)/n = \omega_1 + x_{11}(n + 1) \quad (2)$$

The anharmonicity constant, x_{11}, is the slope of the plot $\nu(n)/n$ versus n, while the harmonic frequency, ω_1, can be obtained from the difference between the intercept and the slope of the same plot. At ambient pressure, the values calculated for the anharmonicity constant and the harmonic frequency of the $\nu_1(A_1)$ mode of the MnO_4^- ion in a KBr host lattice are −0.89 and 846.8 cm^{-1}, respectively (Table 5). These values are in excellent agreement with those reported by Maksimova et al.[9]

TABLE 2: Pressure Sensitivities for the $\nu_1(A_1)$ Overtones and the $n\nu_1 + \nu_3$ Combination Bands of the MnO_4^- Anion in a KBr Matrix

ν (cm^{-1})	$d\nu/dP$ (cm^{-1} $kbar^{-1}$)	assignment
1689	0.64	$2\nu_1(A_1)$
2531	0.98	$3\nu_1(A_1)$
3370	1.3	$4\nu_1(A_1)$
1765	0.80	$\nu_1 + \nu_3$
2606	1.11	$2\nu_1 + \nu_3$

Resonance Raman Spectra of the MnO_4^- Anion Isolated in a Potassium Perchlorate Matrix. The structure of $KClO_4$, which has unit cell parameters $a = 8.866$, $b = 5.666$, and $c = 7.254$ Å, is described by the space group D_{2h}^{16} (*Pnma*) with four units in the primitive cell ($Z = 4$). The tetrahedral ClO_4^- species and K^+ ions are situated on C_s symmetry sites. Through the use of the correlation diagram of the free perchlorate ion symmetry species under T_d symmetry to the species under site group symmetry C_s and factor group symmetry D_{2h}, the following splittings can be predicted:[29] (i) the A_1 mode is not affected by site splitting, because it is nondegenerate, but it should split into four modes, A_g, B_{2g}, B_{1u}, and B_{3u}, under the influence of the D_{2h} factor group. The splitting results in two Raman- and two infrared-active bands. (ii) The E mode is split into two bands (A′ and A″) by site group splitting, and each of these modes should further split into four by factor group splitting. Therefore, four Raman (A_g, B_{2g}, B_{1g}, and B_{3g}) and three infrared (B_{3u}, B_{1u}, and B_{2u}) bands should be observed for the E mode. (iii) Both T_2 vibrations split into three bands (2A′ and A″) by site group splitting, and each of these bands should further split into four components by factor group splitting. As a result, six Raman modes and five infrared modes should be observed for the T_2 vibrations.

Although the correlation diagram of the $KClO_4$ crystal predicts six Raman modes for the $\nu_4(T_2)$ vibration, only three Raman modes were detected, as illustrated in the upper left-hand trace of Figure 6. For the $\nu_3(T_2)$ vibration, three components were observed, located at 1087, 1124, and 1144 cm^{-1}. The first two peaks exhibited shoulders at 1068 and 1118 cm^{-1}, respectively. No splitting was observed for the $\nu_2(E)$ mode. The shoulder appearing at 923 cm^{-1} could be attributed to the first overtone of the $\nu_2(E)$ mode. In addition, the shoulder at 936 cm^{-1} could be assigned to the $\nu_1(A)$ mode.

Potassium permanganate and potassium perchlorate structures are isomorphous, and consequently, it is possible to replace any of the four perchlorate ions in the unit cell with a permanganate ion to provide a site symmetry different from the cubic KBr. The isomorphous isolation method offers the advantage that the vibrational spectrum can be predicted using the site group analysis instead of the unit cell group. When this method is employed, the collective crystal effects are suppressed.

The Raman spectrum in the range 300−1200 cm^{-1} (Figure 6b) shows the bands assigned to the MnO_4^- ion located at ~843.6, 390, and 353 cm^{-1}. The first four overtones of the $\nu_1(A)$ mode were detected. The Raman bands assigned to the $KClO_4$ matrix are shifted slightly toward lower wavenumbers with respect to pure $KClO_4$.

From Figure 7, the application of the external pressure on the MnO_4^- ion in the $KClO_4$ matrix leads to overall linear shifts toward higher wavenumbers of the Raman bands assigned to

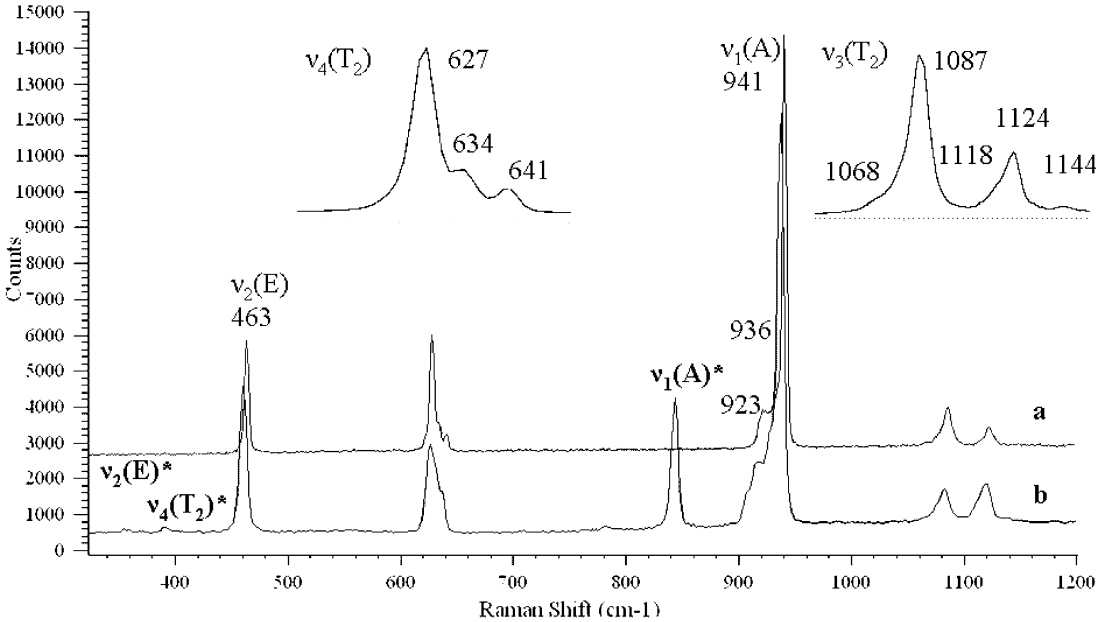

Figure 6. Vibrational modes of (a) the $KClO_4$ crystal and (b) the MnO_4^- anion isolated in a $KClO_4$ host matrix at ambient pressure. The bands and the assignments of the doped MnO_4^- anion are indicated with an asterisk.

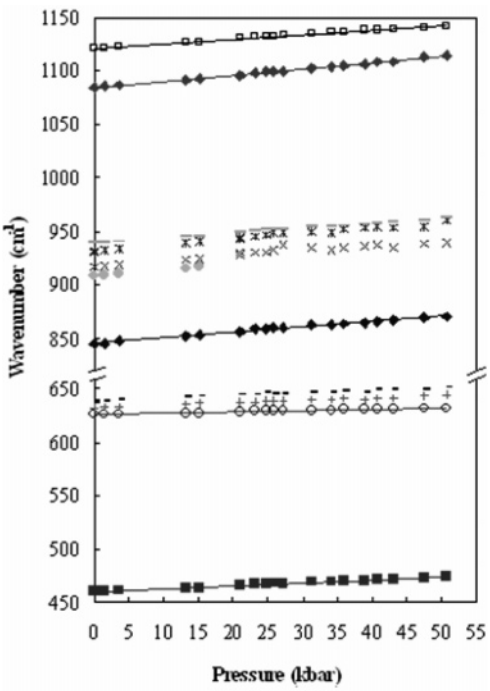

Figure 7. Raman wavenumber versus pressure for the MnO_4^- anion isolated in a $KClO_4$ matrix: (◆) $\nu_1(A_1)/MnO_4^-$, (■) $\nu_2(E)/ClO_4^-$, (○) $\nu_4(T_2)/ClO_4^-$, (+) $\nu_4(T_2)/ClO_4^-$, (−) $\nu_4(T_2)/ClO_4^-$, (gray tilted square) $\nu_1(A_1)/ClO_4^-$, (×) $\nu_1(A_1)/ClO_4^-$, (∗) $\nu_1(A_1)/ClO_4^-$, (gray solid line) $\nu_1(A_1)/ClO_4^-$, (dark-gray tilted square) $\nu_3(T_2)/ClO_4^-$, (□) $\nu_3(T_2)/ClO_4^-$.

the $\nu_1(A_1)$ vibration mode of the MnO_4^- anion and to the normal modes of the host matrix. There is no pressure-induced phase transition in the $KClO_4$ crystal under the experimental conditions used in this study, in agreement with the results of Pistorius.[30] The transition point from an ordered $KClO_4$ orthorhombic (*Pnma*) structure to a partly disordered $KClO_4$ cubic (*Fm*3*m*) one increases from 296 °C at atmospheric pressure to 566 °C at 11.3 kbar, when explosive decomposition occurs.

Khodadoost et al.[21] have reported that when the pressure is increased up to 106 kbar the ground- and excited-state vibrational frequencies of the MnO_4^- ion in a $KClO_4$ matrix increase linearly. The dν/dP value and the intercept for the pressure dependence of the ground-electronic-state vibrational frequency were estimated at 0.505 cm^{-1} kbar^{-1} and 845 cm^{-1}, respectively. The values of the pressure sensitivities dν/dP of the vibrational modes of the MnO_4^- anion and of the $KClO_4$ environment are given in Table 3 and range from 0.13 to 0.59 cm^{-1} kbar^{-1}. The value obtained for the pressure dependence of the $\nu_1(A_1)$ mode of the MnO_4^- ion in the $KClO_4$ host matrix is in excellent agreement with the 0.505 cm^{-1} kbar^{-1} value obtained by Khodadoost.

TABLE 3: Pressure Sensitivities of Observed Raman Bands of the MnO_4^- Anion in a $KClO_4$ Host Lattice

ν (cm^{-1})	dν/dP (cm^{-1} kbar^{-1})	assignment
844	0.51	$\nu_1(A_1)/MnO_4^-$
460	0.28	$\nu_2(E)/ClO_4^-$
626	0.13	$\nu_4(T_2)/ClO_4^-$
632	0.22	$\nu_4(T_2)/ClO_4^-$
638	0.24	$\nu_4(T_2)/ClO_4^-$
908	0.56	$\nu_1(A_1)/ClO_4^-$
917	0.46	$\nu_1(A_1)/ClO_4^-$
931	0.53	$\nu_1(A_1)/ClO_4^-$
939	0.46	$\nu_1(A_1)/ClO_4^-$
1084	0.59	$\nu_3(T_2)/ClO_4^-$
1121	0.43	$\nu_3(T_2)/ClO_4^-$

Three overtones of the $\nu_1(A_1)$ mode of the MnO_4^- anion were also observed for the perchlorate matrix and measured up to ~50 kbar, Figure 8. Table 4 shows the Raman wavenumbers and the pressure dependences of the $\nu_1(A_1)$ overtones for the MnO_4^- anion trapped in a $KClO_4$ matrix. As expected, no discontinuities or changes in slopes of the ν versus P plots were observed.

Through the use of the procedure described above (eq 2), the anharmonicity constant and harmonic frequency were obtained. The values, at ambient pressure, were −0.85 and 845.9 cm^{-1}, respectively. Figure 9 illustrates the pressure dependence of the harmonic frequencies of MnO_4^- ion in both host lattices. The anharmonicity constants decrease slightly with increasing pressure, while the harmonic frequencies increase.

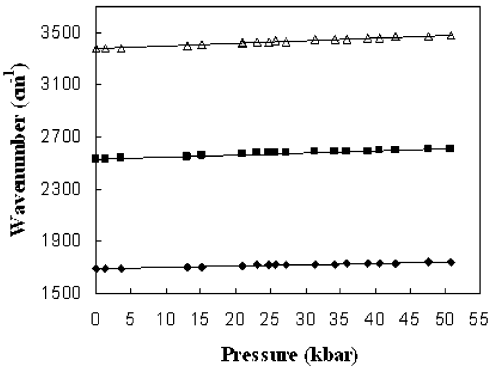

Figure 8. Pressure dependence of $n\nu_1$ overtones of the MnO_4^- anion isolated in a $KClO_4$ matrix: (◆) $2\nu_1(A_1)$, (■) $3\nu_1(A_1)$, (△) $4\nu_1(A_1)$.

TABLE 4: Pressure Sensitivities of the $\nu_1(A_1)$ Mode and Its Observed Overtones for the MnO_4^- Anion Trapped in a $KClO_4$ Host Lattice

ν (cm^{-1})	$d\nu/dP$ (cm^{-1} $kbar^{-1}$)	assignment
1690	1.04	$2\nu_1(A_1)/MnO_4^-$
2533	1.57	$3\nu_1(A_1)/MnO_4^-$
3373	2.07	$4\nu_1(A_1)/MnO_4^-$

TABLE 5: Anharmonicity Constants and Harmonic Frequencies for the $\nu_1(A_1)$ Mode of the MnO_4^- Anion in Different Environments at Ambient Pressure

	compound	x_{11} (cm^{-1})	ω_1 (cm^{-1})	ref
1	MnO_4^- aq soln	−1.0	839.5	6
2	MnO_4^- solid	−1.1	845.5	6
3	$BaMnO_4$	−3.3	828.0	16
4	MnO_4^-/RbBr	−1.22	846.8	16
5	$MnO_2{}^{18}O_2^-$/RbBr	−1.18	817.8	16
6	$Mn^{18}O_4^-$/RbBr	−0.99	798.4	16
7	$MnO_4^-/(Bu_4N)$	−1.0	836.0	31
8	MnO_4^-/sodalite	−1.3	*b*	18
9	MnO_4^-/Ph_4P	−1.3	837.9	19
10	MnO_4^-/KBr	−0.95	847.6	9
11	MnO_4^-/KBr	−0.89	846.8	this work[a]
12	$MnO_4^-/KClO_4$	−0.88	848.6	19
13	$MnO_4^-/KClO_4$	−0.85	845.9	this work[a]

[a] Values were obtained using the progression $n\nu_1$, $n = 1-5$. The resonance Raman spectrum was recorded on a microscope slide. [b] Not available.

Table 5 summarizes the values calculated for the anharmonicity constant and harmonic frequency of the $\nu_1(A_1)$ mode of the MnO_4^- ion trapped in a KBr and a $KClO_4$ matrix, together with those reported in the literature for the permanganate ion in aqueous solution, as a solid, and in different crystalline environments.

The wavenumbers of the fundamental modes of the permanganate anion in both KBr and $KClO_4$ lattices are higher than are those in the pure $KMnO_4$ crystal due to the increased compression of the MnO_4^- ion after its insertion into the host matrix. The volume of the unit cell of KBr is about 36% smaller than that of $KMnO_4$, so a shift toward higher wavenumbers is expected. The absence of the splitting of the band located at 925 cm^{-1} in the Raman spectra of the MnO_4^- ion in a KBr matrix indicates that the tetrahedral symmetry of the permanganate ion is maintained after its insertion into the KBr host lattice. The unit cell volume of the $KClO_4$ crystal is around 6% smaller than that of pure $KMnO_4$. Moreover, on comparison of the Raman spectra at ambient pressure of the MnO_4^- ion in each of the matrices studied, it can be observed that the $\nu_1(A_1)$ mode of the MnO_4^- ion is slightly higher in the KBr host matrix than that in the $KClO_4$ environment. This shift is due to the higher compression of the MnO_4^- ion in KBr than in the $KClO_4$ matrix. On comparison of the pressure dependences of the totally symmetric $\nu_1(A)$ mode of the MnO_4^- ion in both matrices, it can be observed that the $d\nu/dP$ value in the KBr lattice is smaller than that in the $KClO_4$ matrix, 0.32 and 0.51 cm^{-1} $kbar^{-1}$, respectively. A possible explanation could be that, at ambient pressure, the MnO_4^- anion trapped in KBr is already more compressed than it is $KClO_4$, which could lead to the smaller pressure sensitivity.

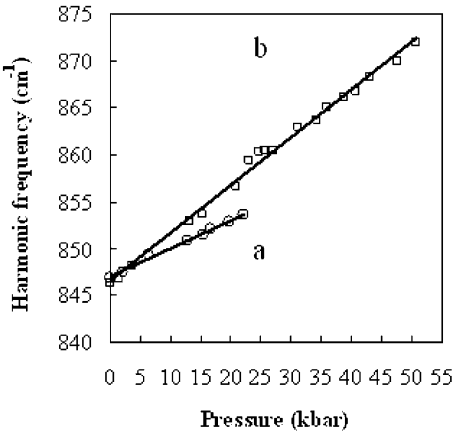

Figure 9. Harmonic frequency as a function of pressure for the MnO_4^- anion in (a) KBr and (b) $KClO_4$ host lattices.

Jubert and Varetti[16] have calculated the anharmonicity constant and harmonic frequency, at ambient pressure, for other manganate salts. According to their study, the following trends can be observed: (i) the anharmonicity constant for manganate(VII) surrounded by singly charged cations is relatively insensitive to the environment (Table 5, rows 1, 2, 4, and 7), (ii) with increasing cation charge, the anharmonicity constant and the harmonic frequency decrease (Table 5, rows 2 and 3), and (iii) as the number of ^{18}O atoms in the ion increases, the anharmonicity constant becomes higher while the harmonic frequency decreases (Table 5, rows 4−6).

Clark and Dines[19] have observed that it is very difficult to correlate the values of the anharmonicity constant with the size of the host matrix, due to the relative insensitivity of this parameter. However, it was found that on increasing the size of the host matrix the harmonic frequency decreases significantly (Table 5, rows 7 and 12). From this reasoning, upon application of an external pressure, and thus causing a decrease in cell volume, the harmonic frequency would be expected to increase, as shown in Figure 9. The values for the anharmonicity constant are very similar for both matrices, while the harmonic frequency of the MnO_4^- ion in KBr is slightly higher than that in the $KClO_4$ host matrix.

Conclusions

Resonance Raman spectra of the MnO_4^- ion embedded in KBr and $KClO_4$ host matrices have been investigated under hydrostatic pressure up to ∼50 kbar, and the anharmonicity constants and the harmonic frequencies for the totally symmetric stretching $\nu_1(A_1)$ mode of the dopant ion have been obtained. The effect of the pressure-induced phase transition of the KBr lattice on the permanganate Raman spectrum was observed at ∼24 kbar. This phase transition was indicated by a sudden change in the slope of the $\nu_1(A_1)$ mode of the permanganate anion as function of pressure, the appearance of a second peak, and the disappearance of several fundamentals and overtones. The observed changes are reversed upon pressure release. As

expected, no pressure-driven phase transition was observed in the case of the $KClO_4$ host matrix. For both crystals, the increase of pressure leads to an increase of the harmonic frequencies, as expected,[32] and to a slight decrease of the anharmonicity constants.

Acknowledgment. This research was supported by grants from the Natural Sciences and Engineering Research Council of Canada and the Fonds de Recherché sur la Nature et les Technologies Québec. The Laboratory of Materials Characterization at the Université de Montréal is thanked for the use of the Renishaw Raman spectrometer.

References and Notes

(1) Hendra, P. J. *Spectrochim. Acta, Part A* **1968**, *24*, 125−129.
(2) Hendra, P. J.; Le Barazer, P.; Crookell, A. *J. Raman Spectrosc.* **1989**, *20*, 35−40.
(3) Kiefer, W.; Bernstein, H. J. *Appl. Spectrosc.* **1971**, *25*, 609−613.
(4) Zimmerer, N.; Kiefer, W. *Appl. Spectrosc.* **1974**, *28*, 279−281.
(5) Kiefer, W.; Bernstein, H. J. *Chem. Phys. Lett.* **1971**, *8*, 381−383.
(6) Kiefer, W.; Bernstein, H. J. *Mol. Phys.* **1972**, *23*, 835−851.
(7) Hallam, H. E. *Vibrational Spectroscopy of Trapped Species; Infrared and Raman Studies of Matrix-Isolated Molecules, Radicals and Ions*; J. Wiley: London, New York, 1973.
(8) Hagemann, H.; Ravi Sekhar, Y.; Bill, H. *J. Chem. Educ.* **1987**, *64*, 456−458.
(9) Maksimova, T. I.; Reshetnyak, N. B. *Sov. Phys. Solid State* **1978**, *20*, 669−671.
(10) Maksimova, T. I.; Reshetnyak, N. B. *Sov. Phys. Solid State* **1979**, *21*, 1540−1543.
(11) Rebane, L. A.; Khaav, A. A. *Sov. Phys. Solid State* **1986**, *28*, 574−578.
(12) Clark, R. J. H.; Cobbold, D. G.; Stewart, B. *Chem. Phys. Lett.* **1980,** *69*, 488−490.
(13) Clark, R. J. H.; Stewart, B. *J. Am. Chem. Soc.* **1981**, *103*, 6593−6599.
(14) Taiti, C.; Foggi, P.; Torre, R.; Schettino, V. *Chem. Phys. Lett.* **1992**, *199*, 417−422.
(15) Taiti, C.; Foggi, P.; Signorini, G. F.; Schettino, V. *Chem. Phys. Lett.* **1993,** *212*, 283−288.
(16) Jubert, A. H.; Varetti, E. L. *J. Mol. Struct.* **1982**, *79*, 285−288.
(17) Martin, T. P.; Onari, S. *Phys. Rev. B* **1977**, *15*, 1093−1099.
(18) Srdanov, V. I.; Harrison, W. T. A.; Gier, T. E.; Stucky, G. D.; Popitsch, A.; Gatterer, K.; Markgraber, D.; Fritzer, H. P. *J. Phys. Chem.* **1994**, *98*, 4673−4676.
(19) Clark, R. J. H.; Dines, T. J. *J. Chem. Soc., Faraday Trans.* **1982**, *78*, 723−728.
(20) Khanna, R. K.; Stranz, D. D. *Spectrochim. Acta, Part A* **1980**, *36*, 387−388.
(21) Khodadoost, B.; Lee, S. A.; Page, J. B.; Hanson, R. C. *Phys. Rev. B* **1988**, *38*, 5288−5295.
(22) *GRAMS/32 Spectral Notebase*, version 4.14; Galactic Industries Corporation: 1991−1996.
(23) Mao, H. K.; Bell, P. M.; Shaner, J. W.; Steinberg, D. J. *J. Appl. Phys.* **1978**, *49*, 3276−3283.
(24) Bassett, W. A.; Takahashi, T.; Campbell, J. K. *Trans. Am. Crystallogr. Soc.* **1969**, *5*, 93−103.
(25) Singh, S.; Singh, R. K.; Singh, B. P. In *Solid State Physics*, Proceedings of the 41st DAE Solid State Physics Symposium, India, 1999; pp 345−346.
(26) Slater, J. C. *Phys. Rev.* **1924**, *23*, 488−500.
(27) Jacobs, R. B. *Phys. Rev.* **1938**, *54*, 468−474.
(28) Herzberg, G. *Molecular Spectra and Molecular Structure II. Infrared and Raman Spectra of Polyatomic Molecules*; D. Van Nostrand Company: Princeton, NJ, 1966.
(29) Toupry, N.; Poulet, H.; Le Postollec, M.; Pick, R. M.; Yvinec, M. *J. Raman Spectrosc.* **1983**, *14*, 166−177.
(30) Pistorius, C. W. F. T. *J. Phys. Chem. Solids* **1970**, *31*, 385−389.
(31) Homborg, H.; Preetz, W. *Spectrochim. Acta, Part A* **1976**, *32*, 709−718.
(32) Sherman, W. F.; Wilkinson, G. R., *Advances in Infrared and Raman Spectroscopy*; Clark, R. J. H., Hester, R. E., Eds.; Heyden, London, 1983.